Calcium EXAFS Establishes the Mn-Ca Cluster in the Oxygen-Evolving Complex of Photosystem II[†]

Roehl M. Cinco,[‡,§] Karen L. McFarlane Holman,[‡,||] John H. Robblee,[§,‡,⊥] Junko Yano,[§,‡] Shelly A. Pizarro,[§,‡,#] Emanuele Bellacchio,[‡] Kenneth Sauer,[§,‡] and Vittal K. Yachandra*,[‡]

Physical Biosciences Division, Melvin Calvin Laboratory, Lawrence Berkeley National Laboratory, Berkeley, California 94720-5230, and Department of Chemistry, University of California, Berkeley, California 94720-5230

Received August 5, 2002; Revised Manuscript Received September 19, 2002

ABSTRACT: The proximity of Ca to the Mn cluster of the photosynthetic water-oxidation complex is demonstrated by X-ray absorption spectroscopy. We have collected EXAFS data at the Ca K-edge using active PS II membrane samples that contain approximately 2 Ca per 4 Mn. These samples are much less perturbed than previously investigated Sr-substituted samples, which were prepared after Ca depletion. The new Ca EXAFS clearly shows backscattering from Mn at 3.4 Å, a distance that agrees with that surmised from previously recorded Mn EXAFS. This result is also consistent with earlier related experiments at the Sr K-edge, using samples that contained functional Sr, that show Mn is ~3.5 Å distant from Sr. The totality of the evidence clearly advances the notion that the catalytic center of oxygen evolution is a Mn-Ca heteronuclear cluster.

Calcium is essential as a cofactor for photosynthetic oxygen evolution in green plants and algae. Together with another cofactor, chloride, calcium is involved in a four-manganese cluster to catalyze the light-driven oxidation of water into dioxygen, protons, and electrons for carbon fixation (*1–4*). The water-splitting reaction occurs within the oxygen-evolving complex (OEC[1]) of photosystem II (PS II), located in the thylakoid membranes of green plants, cyanobacteria, and algae. It is crucial to study the Ca cofactor, as recent mechanisms of oxygen evolution (*5–9*) have proposed roles for Ca (and Cl) that require it to be located near the Mn cluster. Studies on photoactivation and assembly of the Mn cluster also implicate a requirement for nearby Ca in the light-induced assembly of the water-oxidizing complex (*10–12*).

While the Mn cluster has been extensively researched, mainly by X-ray absorption spectroscopy (XAS) (*13–16*) and electron paramagnetic resonance (EPR) techniques (*17*), the calcium cofactor has been comparatively less studied (*1, 18, 19*). This is explained by the lack of spectroscopic handles for Ca compared to Mn. Previous work on the structure of the binding site of the Ca cofactor has mainly consisted of studies involving Ca depletion (*20–23*) or substituting other metals (*24*), including strontium, manganese, or terbium for the cofactor (*25–28*). FTIR spectroscopy suggests a carboxylate bridge between Mn and Ca in PS II (*29*), but a later study disputes this finding (*30*). Structural information about the binding site of the Ca cofactor has been obtained recently through extended X-ray absorption fine structure (EXAFS) experiments on strontium-substituted PS II membranes (*31–33*) and through [87]Sr ESEEM (electron spin-echo envelope modulation) spectroscopy (R. D. Britt, personal communication, 2002).

Strontium is the only metal ion that replaces calcium and still maintains oxygen-evolving activity (up to 40% at saturating light levels) (*34*). Earlier efforts using Mn EXAFS on Sr-reactivated PS II (*31*) implicated a 3.5 Å distance between the Mn cluster and Sr. More recently, Sr EXAFS on similar samples confirms this finding of a 3.5 Å distance between Sr and Mn in the OEC (*32*). The finding is based on the presence of a second Fourier peak in the Sr EXAFS from intact Sr-substituted PS II that is absent from inactive, hydroxylamine-treated PS II (Figure 2, inset). The Fourier peak II is found to fit best to two Mn at 3.5 Å rather than to lighter atoms such as carbon. Further, the use of polarized Sr EXAFS has shown this peak to be dichroic (*35*) and found an average orientation for the two Sr–Mn vectors (*36*). While Sr substitution in PS II and XAS have yielded valuable insight into the Ca cofactor, it is nevertheless an indirect

* To whom correspondence should be addressed. Telephone (510) 486-4330. Fax (510) 486-6059. E-mail: vkyachandra@lbl.gov.

‡ Physical Biosciences Division, Lawrence Berkeley National Laboratory.

§ Department of Chemistry, University of California, Berkeley.

|| Present address: Department of Chemistry, Willamette University, Salem, OR 97301.

⊥ Present address: Department of Chemistry, MIT, Cambridge, MA 02139.

Present address: Sandia National Laboratories, Biosystems Research Department, Livermore, CA 94551.

[1] Abbreviations: Chl, chlorophyll; EPR, electron paramagnetic resonance; EXAFS, extended X-ray absorption fine structure; FT, Fourier transform; LHC II, light-harvesting complex II; MLS, multiline EPR signal; OEC, oxygen evolving complex; PS II, photosystem II; XANES, X-ray absorption near edge structure; XAS, X-ray absorption spectroscopy.

method, requiring treatments such as low-pH Ca depletion (*20, 21*) and Sr reconstitution (*26, 31, 34, 35*).

XAS studies on biological Ca-containing samples have been reported (*37, 38*), including applications to milk Ca phosphate (*39*) and the Ca-binding protein troponin (*40*). To date, though, calcium in PS II has not been directly studied with XAS because of several daunting experimental challenges. First, compared with Mn or Sr, the X-ray fluorescence yield of Ca is lower (*41*), making signal detection difficult. Second, the X-ray energies involved (3.6−4.5 keV) are attenuated significantly by air and regular cryostat windows and other materials used in conventional hard X-ray EXAFS studies. Third, the low concentration of Ca in PS II ($\leq$60 ppm by weight) means that, for biochemical sample preparation, adventitious Ca contamination is a major problem. Extreme care must be taken to remove such extraneous Ca from glassware, solutions, and PS II samples, because nonspecific Ca would contribute to the EXAFS signal, diluting the desired signal from the OEC. Finally, biochemical studies have shown that higher plants have two types of Ca bound to PS II membrane fragments (*20, 42−44*). One of these Ca seems to be bound tightly to the light-harvesting complex II (LHC II) (*45, 46*) while the other, more loosely bound Ca is important for oxygen evolution (*22*). Any Ca EXAFS experiment will measure the averaged signal from these two types.

Despite these obstacles, the ultimate goal remains to probe the Ca cofactor directly. In the first use in photosynthetic systems, we employed Ca K-edge EXAFS on spinach PS II samples containing ~2 Ca per reaction center to detect any neighboring Mn within 4 Å. This technique was analogous to the Sr EXAFS studies done earlier (*32*) in being element-specific, but directly focused on the cofactor binding site in native PS II, requiring no potentially harsh treatments, such as Ca depletion or Sr substitution. The new Ca EXAFS application to PS II clearly shows that Mn is present at 3.4 Å and definitively indicates the proximity of the calcium cofactor to the Mn cluster of oxygen-evolving photosystem II.

EXPERIMENTAL PROCEDURES

Sample Preparation. PS II membrane fragments were prepared as BBY particles from spinach (*47, 48*). The oxygen-evolving activities ranged from 300 to 400 μmol O_2/ mg chlorophyll (Chl)/h, measured as described earlier (*32*). The native PS II samples were stored and frozen in sucrose buffer containing 0.4 M sucrose, 50 mM 2-(*N*-morpholino)-ethanesulfonic acid (MES), 30 mM NaCl, and 5 mM $MgCl_2$ at pH 6.5 and −20 °C. Glassware, utensils, and plasticware were acid-washed with dilute HCl (10%) and rinsed with deionized water, while Ca-free buffers were treated with Chelex-100 chelator resin (Bio-Rad). To remove Ca contamination from the PS II membranes and bring the level down to two Ca per PS II, they were stirred slowly with Chelex-100 resin (1 g resin per 1 mg Chl) in a sucrose-free buffer containing 25 mM MES, 30 mM NaCl, and 3 mM $MgCl_2$ at pH 6.5 (*32, 44, 45*). The final concentration of PS II in the mixture was 0.25 mg Chl/mL. After 1 h of gentle stirring, the PS II was separated from the resin by filtration then centrifugation. The membranes were resuspended in sucrose buffer before a final centrifugation step (15 min, 40 000*g*). Samples were taken for O_2 assay, metals quanti-

tation, and EPR characterization. The resulting Chelex-treated pellet was painted onto flat Ca-free plexiglass slabs (16 × 5 × 1.5 mm) and dried in the dark under a stream of dinitrogen at 4 °C (*49, 50*). Six cycles of painting and drying took 12 h to achieve sufficient concentration of Ca per unit volume to be detectable by X-ray fluorescence. After the last layer had dried, the samples were left in the dark for 1 h to poise them in the S_1 state and then frozen in liquid N_2 for storage. All these procedures were done at 4 °C in dim green light.

A control sample was prepared by adding 40 μL of 100 mM NH_2OH (Ca-free) to the layered, Chelex-treated PS II, inactivating it by disrupting the Mn in the OEC (*51, 52*). The control sample was allowed to soak and dry without loss of PS II material before being frozen in liquid N_2. Characterization of the Chelex-treated samples by metals quantitation (Mn, Ca) by inductively coupled plasma with atomic emission spectroscopy (ICP-AES), EPR spectroscopy, and oxygen-evolving activity assays was done as described previously (*32*), before any of our XAS studies.

Ca EXAFS Data Collection and Analysis. The procedures used were guided by those mentioned previously for Sr EXAFS (*32*), but with important modifications. Ca EXAFS experiments were done at the Stanford Synchrotron Radiation Laboratory (SSRL) beamline IV-2 at the Ca K-edge (4.05 keV) in focused mode with a specially modified liquid-He flow cryostat (Oxford Instruments) and a 13-element Ge detector (*53*) for fluorescence detection. A He flight path was installed before the cryostat to maximize incident X-ray flux (I_0, as measured by the He-filled ionization chamber). The cryostat setup incorporated 6−8 μm Kapton entrance windows and 13−25 μm Kapton fluorescence windows facing the Ge detector (with a supporting 70% transmission grid). These windows are much thinner and more delicate than normal materials used for Mn or Sr EXAFS and allowed sufficient transmission of 4.0−4.6 keV incident and 3.6 keV fluorescent X-rays. All windows and other materials used in the incident beam and fluorescent photon path were tested for the presence of Ca with X-ray fluorescence methods, and were found to be Ca-free. This is an important precaution, because Ca is ubiquitous, and most commonly used window materials contain enough contaminating Ca to complicate the experiment with PS II samples. Mylar windows should be avoided because of contaminating antimony (Sb) L-absorption edges near the Ca K-edge. The temperature in the He-filled (1 atm) cryostat was maintained at 100 ± 3 K for data collection to minimize radiation damage and prevent buildup of frozen Ar that can block X-rays from reaching the detector.

Ca EXAFS data were recorded as fluorescence excitation spectra as the incident X-ray energy was scanned from 4.0 to 4.5 keV using a Si[111] double-crystal monochromator. For energy calibration, $Ca(OAc)_2$ was used as a standard, whose edge peak was assigned to 4.05 keV (*40*). To improve the signal-to-noise ratio, 130 scans (20 min each) from three separate samples of intact Chelex-treated PS II were collected, along with 160 scans from four separate inactive (NH_2OH-treated) samples. The X-ray beam illuminated 3−4 spots (10 × 0.8 mm) per sample for 4 h (about 12 scans per spot). The X-ray energy was scanned from 3.81 to 4.02 keV at 10 eV steps, then 1 eV through the range 4.020−4.076 keV, and finally 0.05 Å^{-1} steps from k = 2.05−11.00 Å^{-1} (E_0 = 4.05 keV).

Data analysis was done using the EXAFSPAK suite of programs by Drs. Graham George and Ingrid Pickering (SSRL). Pre-edge background subtraction was done with a first-order polynomial fitted through 4.00−4.01 keV. Background removal in k-space was achieved through a five-domain cubic spline. Monochromator crystal glitches required truncation of the useable k-range to 2.5−10.5 Å^{-1} before Fourier transformation. The Fourier transforms (FT) were done without windowing, but Fourier isolation was performed with a 0.3 Å Gaussian window. For curve fitting, we used the OPT program of EXAFSPAK, with ab initio phase and amplitude functions calculated by the program FEFF 7.02 (University of Washington) (*54, 55*), assuming pairs of atoms at fixed distances (3.4 Å). The scaling factor S_0^2 of 0.9 was used for all fits. Data analysis procedures (such as Fourier filtering, curve fitting with FEFF) were guided by previous studies on Mn and Sr EXAFS from PS II (*31, 32*) and by instructions in the EXAFSPAK manual.

RESULTS

The Chelex treatment of spinach PS II membranes reduced the level to about 2 Ca per 4 Mn per PS II (200 Chl), consistent with previous studies (*44, 45*). From six Chelex treatments of PS II, we found 1.8 ± 0.3 Ca and 3.8 ± 0.7 Mn per PS II (200 Chl). In accord with the earlier findings, the gentle stirring of Chelex with PS II did not harm oxygen-evolving activity. Compared to control rates (before the treatments), oxygen evolution activities from seven trials ranged from 85% to 99%. This again confirmed that there are minimally two Ca per oxygen-evolving PS II in higher plants, but one is sufficient for oxygen evolution (*22, 45*). The samples were also characterized with EPR spectroscopy, by their ability to produce the light-induced multiline signal (MLS) by advance to the S$_2$ state using continuous illumination at 200 K. Generation of the MLS was not affected by Chelex treatment, as comparison of the EPR spectra from control PS II with the Chelex-treated samples showed essentially the same MLS pattern (data not shown). In samples that have undergone a similar 12 h layering process, such as the oriented Sr-reconstituted PS II (*35*), the Mn EXAFS spectra were nearly identical to the isotropic (pelleted) Sr-PS II (*36*). Finally, the Mn EXAFS spectra from a representative Chelex-treated PS II sample (data not shown) resembled native PS II (*31, 56, 57*). These data indicated that the Mn cluster remained intact after the layering process. Care was taken to properly characterize the layered 2 Ca/PS II samples after sample preparation to ensure their integrity before exposure to X-rays in the Ca EXAFS experiments.

Ca EXAFS Results. The Ca EXAFS experiment probed the two Ca present in oxygen-evolving PS II membranes (*45*), but only one is involved in the OEC (*22*). The k-space (k^3-weighted) Ca EXAFS spectra were obtained from the two types of samples. This required the averaging of 130 scans across three separate samples for the intact 2 Ca/PS II, while 160 scans were needed from three inactive samples. After data reduction, the k-space (k^3-weighted) Ca EXAFS spectra are shown in Figure 1. At this stage, subtle but real differences are apparent, notably around $k = 3.7$−4.1, at 9.7 Å^{-1}, and slightly mismatched phases at $k = 6.0$−8.0 Å^{-1}. Only small differences are visible because only one Ca is
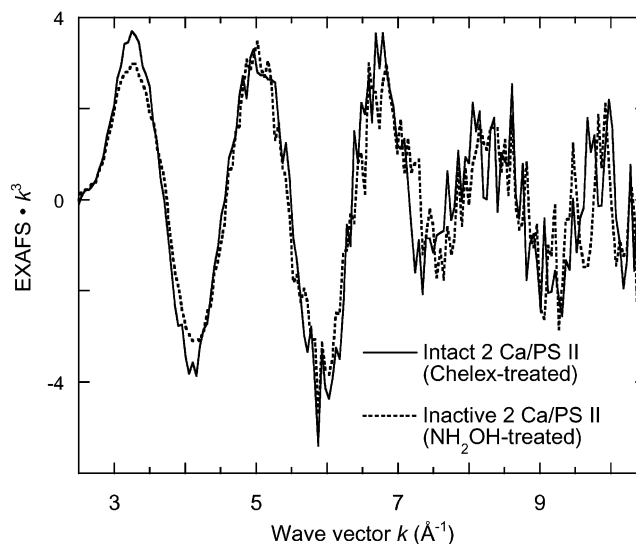

FIGURE 1: Ca EXAFS spectrum in k-space (k^3-weighted) from intact Chelex-treated PS II in the S$_1$ state (—) and the corresponding NH$_2$OH-treated samples (---). After conversion into k-space and background removal (with a five-domain cubic spline), the spectra from two types of samples are presented. These represent the average of 130 scans from intact samples and 160 scans from inactive samples. Subtle but clear and reproducible differences in phase and amplitudes are visible in the range of $k = 3$−4, 6−7, and 9−10, Å^{-1}. These differences become more pronounced when contribution from the extraneous Ca not involved in oxygen evolution is subtracted (data not shown). The differences become more obvious in the Fourier transforms shown in Figure 2.

being affected by the NH$_2$OH treatment. These differences become more pronounced when contribution from the extraneous Ca, not involved in oxygen evolution, is subtracted (data not shown).

The Fourier transforms (FT) of the Ca EXAFS are presented in Figure 2 and make the differences more prominent. The pattern of the FTs is remarkably similar to that in the parallel, earlier Sr EXAFS study (Figure 2 inset) (*32, 35*). The first, dominant Fourier peak is due to coordinating oxygen closest to calcium (5−6 O at 2.4 Å) (*37, 58*). In contrast to the inactive (NH$_2$OH-treated) PS II, the intact 2 Ca/PS II sample showed a second Fourier peak near 'R' ~ 2.9 Å, well above the noise level ('R' ~ 4−10 Å). Fourier peak II was present only in intact Chelex-treated PS II (Figure 2) and so was the focus of Fourier isolation and curve fitting to determine the identity of the neighbors at this distance.

EXAFS Curve Fitting of Peak II. Fourier peak II in Figure 2 was isolated with a Gaussian window (0.3 Å width) from $R = 2.4$−3.5 Å and backtransformed into k-space. The OPT program was used for curve-fitting along with FEFF phases and amplitudes as we varied the coordination number N, the distance R, the Debye−Waller factor σ^2, and ΔE_0. The short range of the data ($\mu R = 1.1$ Å) allowed for only one shell of scattering atoms (Mn, C, O, Cl) to produce unique fits. For Table 1, we fixed the N to best integer values and also tried half-integer steps of Mn from 0.5 to 2.0. As Table 1 shows, the best single-shell fit to peak II was with Mn at 3.4 Å. The fit with O produced an unrealistic, negative Debye−Waller factor σ^2 of −0.0009 Å^2, while the other light atoms (C, Cl) showed increased fitting errors (80% and 30% more than for Mn, respectively).
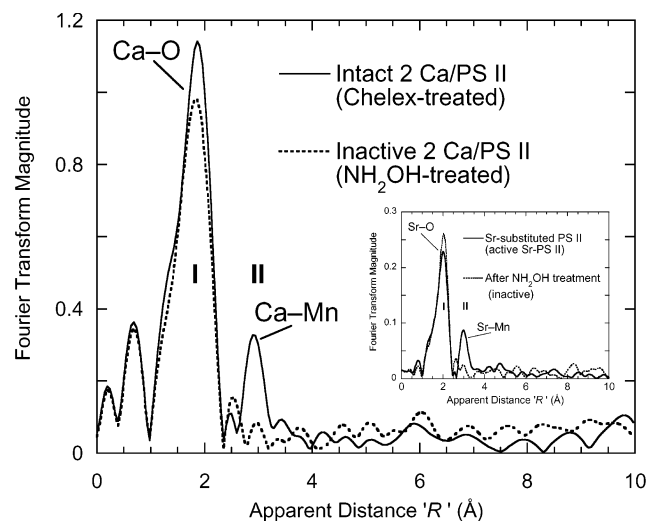
FIGURE 2: Fourier transforms of Ca EXAFS from Chelex-treated, layered samples with 2 Ca/PS II (k^3-weighted, $k = 2.5-10.5$ Å^{-1}). Intact (—) and inactive (---) 2 Ca/PSII samples are shown. These are the FTs of the EXAFS spectra in the previous figure. Apparent distance 'R' is less than the actual distance by about 0.5 Å. The peak at 'R' < 1 Å is an artifact of incomplete background removal. Fourier peak I consists of nearest-neighbor oxygen atoms, while Fourier peak II fits best to Mn scattering and is absent in inactive samples where the Mn cluster is disrupted by NH$_2$OH treatment. The pattern of peaks can be compared to that in the inset. The Fourier transform magnitudes are in arbitrary units. Inset: Fourier transform of Sr EXAFS from isotropic Sr-substituted PS II samples (k^3-weighted, $k = 2.7-11.7$ Å^{-1}). Apparent distance 'R' is less than the actual distance by about 0.5 Å. Fourier peak I consists of nearest-neighbor oxygen atoms while Fourier peak II, which is present in the intact Sr-PS II (—) and absent in inactive samples (---), fits best to Mn scattering atoms. Adapted from an earlier Sr EXAFS study (*32*).

Table 1: Ca EXAFS Fitting Results for Fourier Peak II (Single-Shell)[a]

scatterer	R (Å)	N[b]	σ^2 (Å^2)	ΔE_0 (eV)	F (error)[c]
Mn	3.40	1	0.0085	−9.5	0.71
Mn	3.40	0.5	0.0035	−10.4	1.13
Mn	3.41	1.5	0.0123	−9.9	1.13
Mn	3.41	2.0	0.0155	−9.2	1.76
C	3.45	2	0.0012	−4.0	1.28
Cl	3.50	1	0.0044	−13.8	0.93

[a] Only three parameters were varied during the fitting procedure for each shell. [b] The coordination number N was fixed to the best integer value for each fit, but other half-integer steps of Mn were also tried. [c] The F (error) is the sum of squares of the residuals.

The Ca EXAFS results confirmed the presence of Mn at a close distance (3.4 Å) to the Ca cofactor, in agreement with previous findings by Mn and Sr EXAFS studies (*31, 32*) of PS II in the S$_1$ state. Lighter atoms contributing to the scattering beyond $R \sim 3$ Å were deemed unlikely by the fitting results. However, to fully interpret the results of Mn fitting of the EXAFS data, they must be evaluated in the context of the stoichiometry in these samples: two Ca per PS II.

DISCUSSION

The first use of Ca EXAFS spectroscopy on a photosynthetic enzyme has produced results essentially congruent with those found by other independent methods: Sr EXAFS on Sr-reactivated PS II (*32*) and Mn EXAFS on similar
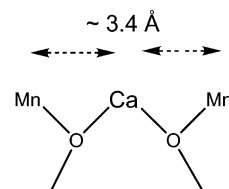

FIGURE 3: Model of Ca-binding site of the oxygen-evolving complex in PS II. From the results of the Ca EXAFS studies on PS II, the Ca cofactor is linked by single-O bridging to two Mn. The oxygens can be provided by water, hydroxyl, or protein residues (carboxylate, phenolate). Other bridging that may be present (single-O or bidentate three-atom) or other ligands to Ca are not depicted for clarity. The arrangement shown here is not unique, as other placements of the two Mn around the Ca are conceivable.

samples (*31*). The characterizations by O$_2$ activity, EPR, and metals quantitation show that the Chelex treatment serves to remove only nonessential Ca and reduce the content to 2 Ca per PS II, without damaging the activity of the OEC. Like the earlier Sr EXAFS, the present Ca EXAFS study has focused on the Ca cofactor of PS II (poised in the S$_1$ state). However, the signal observed here is the composite of the two Ca present in higher plant PS II membranes. One of these Ca is tightly bound in the LHC II complex (*45, 59*), but the other is crucial for oxygen evolution. The EXAFS fitting results must be examined in light of this stoichiometry.

In Figure 2, the Fourier transforms of the Ca EXAFS from intact and inactive 2 Ca/PS II are presented. While there is a slight difference in peak I, the roughly comparable peak heights suggest the Ca binding sites for the two types of samples share similar first coordination shells. Generally, protein calcium coordination has been found to consist of six oxygen ligands, in agreement with our peak I fitting of 5−6 O at 2.4 Å (*37, 58*). However, the most striking contrast between the two types of samples is peak II: visible in the intact sample but absent in inactive PS II. The EXAFS fitting gives $N = 1$ Mn at 3.4 Å for peak II (Table 1). However, only half of the Ca in PS II is located in the OEC, which houses the Mn cluster (*1*). The other half, embedded in the LHC II, is thought to have no metals around it (*45, 59*). Therefore, after correcting for the stoichiometry of Ca in PS II, we obtain the coordination number $N = 2$ for Mn at 3.4 Å. When hydroxylamine is added to the Chelex-treated PS II, the Mn cluster is disrupted from its binding site (*52*), rendering the two Ca−Mn vectors undetectable (longer than 3.4 Å) and explaining the absence of peak II in Figure 2. In this case, both Ca sites are similarly devoid of any nearby metals (out to 4 Å). We have also analyzed the EXAFS data (data not shown) after subtracting the EXAFS of the inactive Ca/PS II (Ca surrounded only by first-shell oxygens) from the intact spectra to remove the contribution from the nonessential Ca, leaving only the signal from the important Ca cofactor. The EXAFS fitting results from these data also clearly favor two Mn neighbors to Ca at 3.4 Å.

The extracted distance of the Ca−Mn vectors (3.4 Å) is shorter than that found by Sr EXAFS (3.5 Å), presumably because of the smaller ionic radius of Ca compared with Sr (*60*). This experiment has directly probed the Ca cofactor in as close to a native system as possible, and the results are summarized in a motif shown in Figure 3. This motif, mentioned in previous studies (*31, 32*), depicts the Ca linked to two Mn by single-O bridging, which can be supplied by

protein residues or water. Only single-oxygen bridging (not bidentate bridges) is likely to provide the required 3.4 Å distance indicated by the Ca EXAFS fitting (*31, 32*). The figure depicts one configuration, and other orientations of the two Mn around the Ca are possible. For clarity, only one single-O bridge is shown between each Ca−Mn pair, but other bridging (single-atom, bidendate, or three-atom) may be present but are not displayed. Our finding will inform and complement the current efforts in other laboratories to obtain a crystallographic structure of the oxygen-evolving complex within photosystem II (*61*).

Researchers have speculated that Ca controls substrate water binding to the catalytic Mn site (*18, 19, 62*) and recent mechanisms have suggested the crucial involvement of the cofactor (*10−12*). Finding the actual role of Ca as the complex goes through the Kok cycle of S-states and the orientation of the Ca−Mn vector, will contribute toward developing a working mechanism of water oxidation. The results from preceding studies using Mn EXAFS (*31*), Sr EXAFS (*32*), and now Ca EXAFS as presented here are mutually consistent and converge toward the conclusion that the calcium cofactor is intimately structurally linked with the Mn cluster in PS II. Taken together, the three methods offer compelling evidence that the catalytic center of photosynthetic oxygen evolution is a heteronuclear Mn-Ca cluster.

ACKNOWLEDGMENT

REFERENCES

1. Debus, R. J. (1992) *Biochim. Biophys. Acta 1102*, 269−352.
2. Britt, R. D. (1996) in *Oxygenic Photosynthesis: The Light Reactions* (Ort, D. R., and Yocum, C. F., Eds.) pp 137−164, Kluwer Academic Publishers, Dordrecht, The Netherlands.
3. Diner, B. A., and Babcock, G. T. (1996) in *Oxygenic Photosynthesis: The Light Reactions* (Ort, D. R., and Yocum, C. F., Eds.) pp 213−247, Kluwer Academic Publishers, Dordrecht, The Netherlands.
4. Yachandra, V. K., Sauer, K., and Klein, M. P. (1996) *Chem. Rev. 96*, 2927−2950.
5. Limburg, J., Vrettos, J. S., Liable-Sands, L. M., Rheingold, A. L., Crabtree, R. H., and Brudvig, G. W. (1999) *Science 283*, 524−527.
6. Limburg, J., Szalai, V. A., and Brudvig, G. W. (1999) *J. Chem. Soc., Dalton Trans.* 1353−1361.
7. Tommos, C., and Babcock, G. T. (1998) *Acc. Chem. Res. 31*, 18−25.
8. Renger, G. (1997) *Physiol. Plant 100*, 828−841.
9. Siegbahn, P. E. M. (2000) *Inorg. Chem. 39*, 2923−2935.
10. Ananyev, G. M., and Dismukes, G. C. (1997) *Biochemistry 36*, 11342−11350.
11. Ananyev, G. M., and Dismukes, G. C. (1996) *Biochemistry 35*, 14608−14617.
12. Ananyev, G. M., and Dismukes, G. C. (1996) *Biochemistry 35*, 4102−4109.
13. Robblee, J. H., Cinco, R. M., and Yachandra, V. K. (2001) *Biochim. Biophys. Acta 1503*, 7−23.
14. Schiller, H., Dittmer, J., Iuzzolino, L., Dörner, W., Meyer-Klaucke, W., Solé, V. A., Nolting, H.-F., and Dau, H. (1998) *Biochemistry 37*, 7340−7350.
15. MacLachlan, D. J., Hallahan, B. J., Ruffle, S. V., Nugent, J. H. A., Evans, M. C. W., Strange, R. W., and Hasnain, S. S. (1992) *Biochem. J. 285*, 569−576.
16. Penner-Hahn, J. E. (1998) *Struct. Bond. 90*, 1−36.
17. Britt, R. D., Peloquin, J. M., and Campbell, K. A. (2000) *Annu. Rev. Biophy. Biomol. Struct. 29*, 463−495.
18. Boussac, A., and Rutherford, A. W. (1994) *Biochem. Soc. Trans. 22*, 352−358.
19. Yocum, C. F. (1991) *Biochim. Biophys. Acta 1059*, 1−15.
20. Ono, T.-A., and Inoue, Y. (1988) *FEBS Lett. 227*, 147−152.
21. Ono, T.-A., and Inoue, Y. (1989) *Biochim. Biophys. Acta 973*, 443−449.
22. Ädelroth, P., Lindberg, K., and Andréasson, L.-E. (1995) *Biochemistry 34*, 9021−9027.
23. Ono, T.-A., Rompel, A., Mino, H., and Chiba, N. (2001) *Biophys. J. 81*, 1831−1840.
24. Vrettos, J. S., Stone, D. A., and Brudvig, G. W. (2001) *Biochemistry 40*, 7937−7945.
25. Ono, T.-A., and Inoue, Y. (1989) *Arch. Biochem. Biophys. 275*, 440−448.
26. Boussac, A., and Rutherford, A. W. (1988) *Biochemistry 27*, 3476−3483.
27. Booth, P. J., Rutherford, A. W., and Boussac, A. (1996) *Biochim. Biophys. Acta 1277*, 127−134.
28. Hatch, C., Grush, M., Bradley, R., LoBrutto, R., Cramer, S., and Frasch, W. (1995) in *Photosynthesis: from Light to Biosphere* (Mathis, P., Ed.) pp 425−429, Kluwer Academic Publishers, Dordrecht, The Netherlands.
29. Noguchi, T., Ono, T.-A., and Inoue, Y. (1995) *Biochim. Biophys. Acta 1228*, 189−200.
30. Kimura, Y., and Ono, T.-A. (2001) *Biochemistry 40*, 14061−14068.
31. Latimer, M. J., DeRose, V. J., Mukerji, I., Yachandra, V. K., Sauer, K., and Klein, M. P. (1995) *Biochemistry 34*, 10898−10909.
32. Cinco, R. M., Robblee, J. H., Rompel, A., Fernandez, C., Yachandra, V. K., Sauer, K., and Klein, M. P. (1998) *J. Phys. Chem. B 102*, 8248−8256.
33. Riggs-Gelasco, P. J., Mei, R., Ghanotakis, D. F., Yocum, C. F., and Penner-Hahn, J. E. (1996) *J. Am. Chem. Soc. 118*, 2400−2410.
34. Boussac, A., and Rutherford, A. W. (1988) *Chem. Script. 28A*, 123−126.
35. Cinco, R. M., Robblee, J. H., Rompel, A., Fernandez, C., Yachandra, V. K., Sauer, K., and Klein, M. P. (1999) *J. Synchrotron Rad. 6*, 419−420.
36. Cinco, R. M. (1999) Ph.D. Dissertation, LBNL-44753, University of California, Berkeley, CA.
37. Powers, L., Eisenberger, P., and Stamatoff, J. (1978) *Ann. N.Y. Acad. Sci. 307*, 113−124.
38. Powers, L. (1982) *Biochim. Biophys. Acta 683*, 1−38.
39. Holt, C., Hasnain, S. S., and Hukins, D. W. L. (1982) *Biochim. Biophys. Acta 719*, 299−303.
40. Bianconi, A., Giovannelli, A., Gastellani, L., Alema, S., Fasella, P., Oesch, B., and Mobilio, S. (1983) *J. Mol. Biol. 165*, 125−138.
41. *X-Ray Data Booklet*, LBNL/PUB-490, Rev. 2 (2001) (Thompson, A. C., and Vaughan, D., Eds.), Lawrence Berkeley Laboratory, Berkeley, CA.
42. Cammarata, K. V., and Cheniae, G. M. (1987) *Plant Physiol. 84*, 587−595.
43. Shen, J.-R., Satoh, K., and Katoh, S. (1988) *Biochim. Biophys. Acta 933*, 358−364.
44. Katoh, S., Satoh, K., Ohno, T., Chen, J.-R., and Kashino, Y. (1987) in *Progress in Photosynthesis Research* (Biggins, J., Ed.) pp I.5.625−628, Martinus Nijhoff Publishers, Dordrecht, The Netherlands.
45. Han, K.-C., and Katoh, S. (1993) *Plant Cell Physiol. 34*, 585−593.

46. Chen, C., and Cheniae, G. M. (1995) in *Photosynthesis: from Light to Biosphere* (Mathis, P., Ed.) pp 329−332, Kluwer Academic Publishers, Dordrecht, The Netherlands.

47. Berthold, D. A., Babcock, G. T., and Yocum, C. F. (1981) *FEBS Lett. 134*, 231−234.

48. Dunahay, T. G., Staehelin, L. A., Seibert, M., Ogilvie, P. D., and Berg, S. P. (1984) *Biochim. Biophys. Acta 764*, 179−193.

49. Dau, H., Andrews, J. C., Roelofs, T. A., Latimer, M. J., Liang, W., Yachandra, V. K., Sauer, K., and Klein, M. P. (1995) *Biochemistry 34*, 5274−5287.

50. Mukerji, I., Andrews, J. C., DeRose, V. J., Latimer, M. J., Yachandra, V. K., Sauer, K., and Klein, M. P. (1994) *Biochemistry 33*, 9712−21.

51. Miller, A.-F., and Brudvig, G. W. (1990) *Biochemistry 29*, 1385−1392.

52. Miller, A.-F., and Brudvig, G. W. (1989) *Biochemistry 28*, 8181−8190.

53. Cramer, S. P., Tench, O., Yocum, M., and George, G. N. (1988) *Nucl. Instrum. Methods Phys. Res. A 266*, 586−591.

54. Mustre de Leon, J., Rehr, J. J., Zabinsky, S. I., and Albers, R. C. (1991) *Phys. Rev. B 44*, 4146.

55. Zabinsky, S. I., Rehr, J. J., Ankudinov, A., Albers, R. C., and Eller, M. J. (1995) *Phys. Rev. B 52*, 2995−3009.

56. Cinco, R. M., Rompel, A., Visser, H., Aromí, G., Christou, G., Sauer, K., Klein, M. P., and Yachandra, V. K. (1999) *Inorg. Chem. 38*, 5988−5998.

57. DeRose, V. J., Mukerji, I., Latimer, M. J., Yachandra, V. K., Sauer, K., and Klein, M. P. (1994) *J. Am. Chem. Soc. 116*, 5239−5249.

58. Kretsinger, R. H., and Nelson, D. J. (1976) *Coord. Chem. Rev. 18*, 29−124.

59. Chen, C., Kazimir, J., and Cheniae, G. M. (1995) *Biochemistry 34*, 13511−13526.

60. Rees, W. S., Jr. (1994) in *Encyclopedia of Inorganic Chemistry* (King, R. B., Ed.) pp 67−87, John Wiley & Sons, Chichester, U.K.

61. Zouni, A., Witt, H.-T., Kern, J., Fromme, P., Krauss, N., Saenger, W., and Orth, P. (2001) *Nature 409*, 739−743.

62. Yocum, C. F. (1992) in *Manganese Redox Enzymes* (Pecoraro, V. L., Ed.) pp 71−84, VCH Publishers, New York.